

Dielectric and pyroelectric properties of $\text{Ba}_x\text{Sr}_{1-x}\text{TiO}_3$: Quantum effect and phase transition

H. Wu and W. Z. Shen*

Laboratory of Condensed Matter Spectroscopy and Opto-Electronic Physics, Department of Physics, Shanghai Jiao Tong University, 1954 Hua Shan Road, Shanghai 200030, People's Republic of China

(Received 30 December 2005; published 15 March 2006)

We have carried out a detailed investigation on the dielectric and pyroelectric properties in $\text{Ba}_x\text{Sr}_{1-x}\text{TiO}_3$ (BST) throughout the concentration range (x from 0 to 1), with the emphasis on quantum effect and phase transition. The approach was realized by employing the transverse-field Ising model, taking into account the cell volume effect and ferroelectric distortion, to quantitatively explain most of the experimental observation in the literature. Together with the nonzero-field scaling analysis, we have presented a clear picture for the quantum effect in BST with small impurity concentrations and at low temperatures through electric field dependence of the dielectric and pyroelectric characteristics. It is found that, with the increase of concentration, the BST system undergoes the variation from the quantum paraelectric, to quantum ferroelectric, and to classical ferroelectric with the second-order phase transition evolving into the first-order one at concentrations higher than 0.57.

DOI: [10.1103/PhysRevB.73.094115](https://doi.org/10.1103/PhysRevB.73.094115)

PACS number(s): 77.84.Dy, 77.80.Bh, 77.80.-e, 77.70.+a

I. INTRODUCTION

Barium strontium titanate $\text{Ba}_x\text{Sr}_{1-x}\text{TiO}_3$ (BST), one of the most important perovskite ferroelectric solid solution materials, has attracted much attention and been extensively studied for many years not only because of its various applications but also for its interesting properties of dielectric behavior and phase transition.¹⁻⁴ Due to the high dielectric constant, low dielectric loss, and concentration-dependent phase transition temperature in BST, the research interest has been directed to study the feasibility in dynamic random-access memory.⁵ The large change in dielectric susceptibility under a certain electric field allows the development of BST-based high-performance microwave tunable devices.⁶ Since the solid solution can be formed by SrTiO_3 and BaTiO_3 over the whole concentration range, the properties of BST can be tailored continuously from 0 (pure SrTiO_3) to 1 (pure BaTiO_3). However, the studies were mainly focused on the BST solid solution with relatively high impurity concentrations and at a temperature above 100 K. The quantum effect in BST, which plays an important role in small impurity concentrations and under very low temperatures, was neglected in most of the literatures.

As one of the end members of BST, SrTiO_3 is probably the best-known example of the quantum paraelectric with an antiferrodistortive transition around 105 K and its ferroelectric phase transition is suppressed by large quantum fluctuations even at the very low temperature limit of $T \rightarrow 0$.⁷ Consequently the temperature dependence of dielectric susceptibility of SrTiO_3 will deviate from the Curie-Weiss behavior and begin to saturate at very low temperatures without showing the dielectric peak. On the other hand, quantum paraelectrics can be classified as marginal systems at the limit of the stability of the paraelectric phase and small content of impurities such as Ba, Ca, and Pb will weaken the quantum fluctuation and induce a ferroelectric phase transition,⁸ leading to appearance of the dielectric maximum at phase transition temperature T_C .

It is reported that there exists a critical concentration x_C (quantum limit), above which BST system becomes a ferroelectric and T_C will increase with the impurity concentration.⁹⁻¹⁴ Detailed experimental observation has revealed that for impurity concentration far higher than x_C , T_C increases linearly with impurity concentration.⁹⁻¹¹ For impurity concentration slightly higher than x_C , however, T_C will deviate from linear temperature dependence and exhibit the feature proportional to $(x-x_C)^{1/2}$.¹²⁻¹⁴ Despite the extensive experimental investigations on the phase transition of BST, very scarce theoretical researches have been carried out, limiting the clear understanding of the microscopic mechanism in the concentration dependence of the phase transition behavior.

The above arguments suggest the necessary investigations on the quantum effect and phase transition in BST throughout the whole concentration range (x from 0 to 1). Furthermore, the pyroelectric behavior of ferroelectric materials is of great interest in application for low-cost, high-performance thermal imaging systems.¹⁵ Hybrid structures made from ferroelectric single crystal or ceramics of BST are the most promising pyroelectric infrared detectors available.¹⁶ For such an important material as BST solid solution, however, there are few theoretical investigations on the pyroelectric effect, especially for the cases with very small impurity concentrations close to x_C , where the quantum effect plays a key role. As we know, pyroelectric property scales the response of electrical polarization to the temperature variation. Since the polarization is closely related to the phase transition as well as the quantum effect, we expect that the quantum effect and phase transition will have great influence on the pyroelectric properties in BST.

The Landau theory and transverse field Ising model (TIM) are the two most frequently used approaches to treat the ferroelectric characteristics. In comparison with the Landau theory for classical cases, the TIM is an order-disorder model treating the electric field dependence of susceptibility, the interactions of dipole moments, as well as the quantum me-

chanical effects within a unified framework, on the basis of the motion of active ions in the double-well type potential field. In addition, the TIM has also been extended successfully to pure quantum paraelectrics SrTiO₃¹⁷ and EuTiO₃,¹⁸ and deduced the Barret formula¹⁹ that excellently explain the dielectric properties of the quantum paraelectrics. For another end member BaTiO₃, recent nuclear magnetic resonance (NMR) study has revealed the simultaneous presence of the Ti disorder and the soft mode, which lead to a special type of phase transition with both displacive and order-disorder characteristics.²⁰ We have employed successfully the TIM model to quantitatively describe the soft mode behavior in BST throughout the concentration range.²¹ Furthermore, the BST system is expected to be dominated by a large scale of fluctuations in order parameters in the vicinity of T_C . To clearly demonstrate the quantum effect, it is necessary to have a scaling analysis of the dielectric susceptibility under different electric fields in BST with various impurity concentrations. The nonzero-field scaling analysis has the ability to evidence deviations from the classical criticality, as shown in classic ferroelectrics like TGSe.^{22,23} However, such a susceptibility scaling behavior has not been revealed in BST before.

The motivation of the present paper is to employ the useful and simple TIM, together with the nonzero-field scaling analysis, to investigate the dielectric and pyroelectric properties in BST, with the emphasis on the quantum effect and phase transition. By quantitatively explaining all the experimental observation in the literature, we have shown the fundamental dielectric and pyroelectric properties in BST under different concentrations, temperatures, and electric fields, where a clear picture has been given for the microscopic mechanism of the quantum effect and phase transition in BST.

II. THEORETICAL BACKGROUND

The Hamiltonian H for the BST system within the framework of the TIM^{17,18,21} can be expressed as:

$$H = - \sum_i \Omega S_i^x - \frac{1}{2} \sum_{i,j} J_{ij} S_i^z S_j^z - 2E \sum_i \mu S_i^z \quad (1)$$

where Ω is the tunneling frequency to scale the quantum effect, $S_i = \frac{1}{2}$ and $-\frac{1}{2}$ for up and down pseudospins, respectively, $i \neq j$, J_{ij} denotes the nearest-neighbor pseudospin interaction, E represents the external electric field, μ is the effective dipolar moment of each spin, and the summation $\sum_j J_{ij} = J$ covers the nearest neighbors of site i . Due to the different order parameters between the ferroelectric and antiferrodistortive phase transitions, we have not considered

the antiferrodistortive transition in pure SrTiO₃ in the model.

The key point in our treatment of impurity effect in BST within the framework of the TIM under an external electric field E is related to the corrections on the nearest-neighbor pseudospin interaction J . We should take into account the cell volume effect on the nearest-neighbor pseudospin interaction J , since the impurity concentration-dependent J is associated with the phase transition temperature T_C (via $dJ/dx = 4k_B dT_C/dx$), which, according to Ref. 24, varies with the cell volume in BST. The doping of large Ba²⁺ ions will result in lattice expansion, where both the pseudospin density correction and reversed piezoelectric coupling have to be considered for the dielectric and pyroelectric behavior in BST. Similar treatment for the dielectric properties of Ca_xSr_{1-x}TiO₃ has been carried out through piezoelectric coupling to account for lattice collapse due to small Ca²⁺.²⁵

The variation of T_C in BST depends on the cell volume effect with the difference between the Ba and Sr ion structure: $dT_C = (\partial T_C / \partial a)_x da + (\partial T_C / \partial x)_a dx$, with a the lattice parameter in BST. The value of the cell volume effect $(\partial T_C / \partial a)_x$ can be obtained through extending Landau expansion of the free energy by elastic and piezoelectric contributions.²⁶ Reference 24 has reported 7000 K Å⁻¹ for pure SrTiO₃, and by the method similar to that reported in Ref. 24, we obtain a value of 5300 K Å⁻¹ for pure BaTiO₃ by referring to the parameters given in Refs. 27 and 28. $(\partial T_C / \partial x)_a$ describes the pure effect of the solid solution composition, and is found to be -92 K for SrTiO₃ and -186 K for BaTiO₃ by fitting the soft mode experimental data in Ref. 9.

Furthermore, it is well known that for BaTiO₃ ($x=1$), its phase transition is of first order. References 9 and 12 have reported the experimental phenomena of the first order phase transition in BST for high impurity concentrations. With the decrease of Ba concentration x , the phase transition in Ba_xSr_{1-x}TiO₃ will gradually change from first order to second order. In order to explain this, we should also take into account the modification of J under the contribution of concentration-dependent ferroelectric distortion induced by four-body, six-body, and eight-body interactions in the theoretical approach. If we employ the concentration-dependent parameters of f_4 , f_6 and f_8 to characterize the contribution of the four-body, six-body, and eight-body interactions, respectively, the contribution of the ferroelectric distortion to J can be simply described^{21,29} by multiplying a factor of $f(P) = 1 + f_4 P^2 + f_6 P^4 + f_8 P^6$ with P the mean polarization.

As a result, the nearest-neighbor pseudospin interaction J in BST can be described, after considering the different cell volume effects in pure SrTiO₃ and BaTiO₃, as follows:

$$J = \begin{cases} [J_{10} + 4k_B(dT_C/dx)x](1 + f_4 P^2 + f_6 P^4 + f_8 P^6) & 0 \leq x < 0.2 \\ [J_{20} - 4k_B(dT_C/dx)(1-x)](1 + f_4 P^2 + f_6 P^4 + f_8 P^6) & 0.2 \leq x \leq 1.0 \end{cases} \quad (2)$$

TABLE I. Parameters for two end members of $\text{Ba}_x\text{Sr}_{1-x}\text{TiO}_3$.

End members	a (Å)	μ (e Å)	Ω (k_B K)	f_4 (m^4/C^2)	f_6 (m^8/C^4)	f_8 (m^{12}/C^6)
SrTiO_3	3.905 ^a	1.51 ^b	80 ^b	0	0	0
BaTiO_3	4.005 ^a	2.17 ^c	356 ^c	2.6 ^c	16 ^c	-860 ^c

^aExperimental results from Ref. 12.

^bOur yielded data from Ref. 30.

^cReported data in Ref. 29.

where $J_{10}=142k_B$ K (we deduce from the available data in Ref. 30) and $J_{20}=1666k_B$ K²⁹ are the nearest-neighbor pseudospin interactions of pure SrTiO_3 and BaTiO_3 without the effect of the ferroelectric distortion, respectively. The selection of 0.2 is based on the different cell volume effects separated at $x=0.2$ in BST, as reported in Ref. 24.

For the other parameters, BST can be treated as solid solutions of two isomorphous compounds, and the approach describing a solid solution in first approximation as an ideal crystal with the mean values of the parameters appears more adequate,³¹ i.e., the tunneling frequency Ω to scale the quantum effect, the effective dipolar moment μ of each spin, as well as a , f_4 , f_6 , and f_8 , can be determined by Vegard law. Table I lists all the parameters of a , μ , Ω , f_4 , f_6 , and f_8 for the two end members SrTiO_3 and BaTiO_3 , where the values for BST can be obtained simply by linear interpolation.

We, therefore, can apply the mean field approximation on a single ion in dealing with the Hamiltonian H and obtain numerical results of several physically important quantities related to the phase transition in BST as:

$$P = 2N\mu\langle S^z \rangle = 2N\mu \frac{\text{Tr} S^z \exp(-\beta H)}{\text{Tr} \exp(-\beta H)} \quad (3)$$

$$\chi(T, E) = \frac{1}{\epsilon_0} \frac{dP}{dE} \quad (4)$$

$$p(T, E) = \frac{dP}{dT} \quad (5)$$

where $N = \frac{1}{a^3} = \frac{10^{30}}{(3.905+0.1x)^3}$ the pseudospin density modified by impurity doping, $\langle S^z \rangle$ the average of the pseudospin proportional to the electrical polarization, and $\beta = (k_B T)^{-1}$. $\chi(T, E) \equiv \chi_E(T)$ and $p(T, E) \equiv p_E(T)$ are the temperature- and electric field-dependent dielectric susceptibility and pyroelectric coefficient, respectively.

In order to have a comprehensive understanding of the dielectric susceptibility in BST with various impurity concentrations and under different electric fields, and to qualitatively describe the quantum effect in BST, we employ the static nonzero-external-field scaling analysis^{22,23} in the vicinity of critical points by the relations of:

$$\chi_E(T)/\chi_0(T) = f[E\chi_0^\alpha(T)] \quad (6)$$

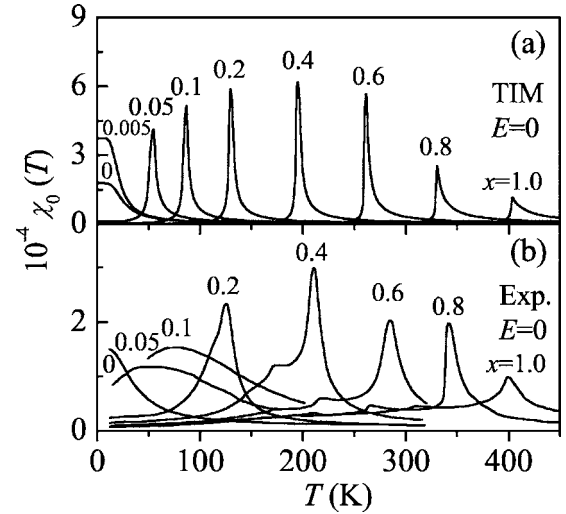


FIG. 1. Temperature dependence of the (a) theoretical and (b) experimental (from Ref. 11) zero-field dielectric susceptibility in $\text{Ba}_x\text{Sr}_{1-x}\text{TiO}_3$ for Ba concentration from 0 to 1.

$$T_m(E) = T_C + AE^{1/\Delta} \quad (7)$$

Here $\alpha = \delta/(\delta-1)$, where the parameter δ is a critical exponent and represents a power law relation of $E \sim P^\delta$ between the external electric field and polarization on the critical isotherm ($T=T_C$). Equation (6) is very convenient for scaling analysis of criticality, because it only contains one fitting parameter a and does not require *a priori* knowledge of T_C . $T_m(E)$ is the temperature of maximum susceptibility $\chi_E(T)$ for a given value of the electric field and it will shift to high temperature with the increase of electric field, A is a concentration-dependent coefficient describing the effect of electric field on $T_m(E)$, and Δ is the gap exponent. As will be shown below, one undoubted merit of the present TIM treatment is its ability to model the scaling behavior in BST. By fitting the yielded dielectric susceptibility with Eqs. (6) and (7) we can get the exponents α , Δ , and the coefficient A , as well as the ratio of Δ to α , all of which can qualitatively describe the quantum effect in BST system. Furthermore, despite the importance of the symmetry and system dimension, they have the same effect on the critical behavior and the exponents in our $\text{Ba}_x\text{Sr}_{1-x}\text{TiO}_3$ bulk system with different impurity concentrations.

III. RESULTS AND DISCUSSION

Figure 1 displays the zero-field ($E=0$) theoretical [Fig. 1(a)] and experimental [Fig. 1(b) from Ref. 11] temperature dependence of the dielectric susceptibility of BST $\chi_0(T)$ with various impurity concentrations. It is clear that the experimental and theoretical dielectric susceptibility show similar feature and most remarkably the temperatures of the dielectric maxima are in good agreement within the whole concentration range, i.e., our present model can reveal quantitatively many basic features of BST despite the remaining deviations. The experimentally observed diffused dielectric behavior in BST with very low concentrations is related with

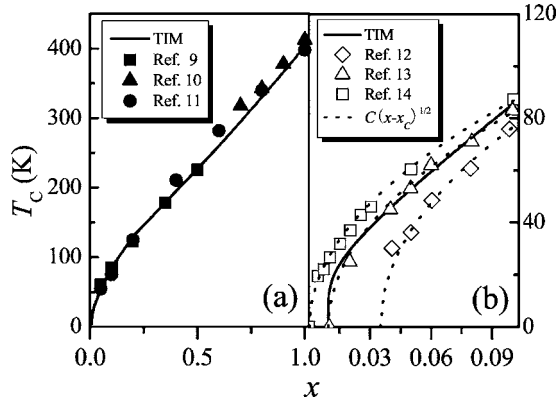


FIG. 2. Phase transition temperature T_C as a function of Ba concentration x for (a) $0 \leq x \leq 1$ and (b) slightly higher than x_C of $0.01 \leq x < 0.1$ with the dashed curves for the empirical relation of $C(x-x_C)^{1/2}$. The scatters are the experimental data in the literature, while the solid curves are the theoretical results under the TIM.

the random field induced domain state in the real material system.¹¹

For SrTiO_3 ($x=0$), the zero-field dielectric susceptibility increases with the decreasing temperature, exhibiting Curie-Weiss behavior in high temperature region, and saturates at very low temperatures. This is due to the strong quantum fluctuation that causes the stabilization of the paraelectric state, resulting in the deviation of the dielectric susceptibility from the Curie-Weiss law. In the case of small Ba content ($x=0.005$), the zero-field dielectric susceptibility exhibits the feature similar to that of pure SrTiO_3 , but the low- T dielectric susceptibility is greatly enhanced. The introduction of impurity will increase the nearest-neighbor interaction and consequently reduce the quantum effect. As a result, the deviation from the Curie-Weiss law is reduced and the saturation reaches a much high value. Further increase of the impurity concentration will induce ferroelectric ordering since the quantum effect is not strong enough to stabilize the paraelectric phase, therefore, there exists a critical concentration x_C , above which, as Fig. 1 shows, the dielectric maximum appears.

Due to the increased nearest-neighbor dipole moment interaction, the dielectric maximum temperature will shift to high temperatures with the increase of the impurity concentration. For high impurity concentrations from $x=0.6$ to 1.0, we note that there is an evident reduction of the dielectric maximum, indicating occurrence of the first-order phase transition. As a result, we can define another threshold concentration x'_C , above which the phase transition is of first order, and our detailed theoretical calculation reveals that x'_C is 0.57. We note that Refs. 9 and 12 have reported an experimental x'_C of ~ 0.2 . Though our theoretical calculation reveals a higher value of x'_C than that in the experiments, possibly due to the deviation of the measured material from the ideal BST crystal and/or the simplicity of our model, our theory has the ability to describe the experimentally observed first-order phase transition in BST at high concentrations. Furthermore, the difference between T_C and T_0 (Curie-Weiss temperature), which is one of the typical features of the first-order phase transition, increases above x'_C , reaching

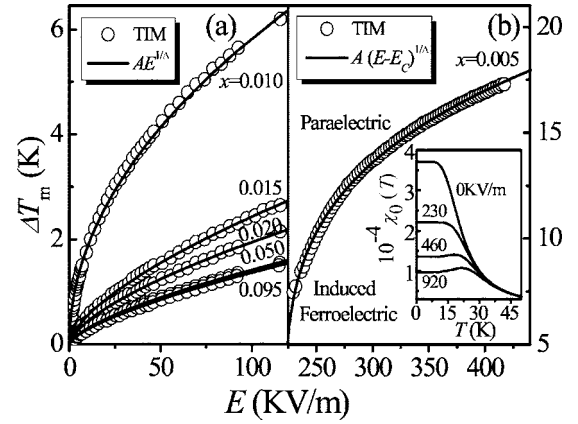


FIG. 3. Electric field dependence of $\Delta T_m(E)$ for (a) x slightly higher than x_C ($0.01 \leq x < 0.10$) and (b) $x < x_C$ ($x=0.005$). The open circles are the theoretical results under the TIM, while the solid curves are the scaling theory fitting. The inset in (b) shows the temperature dependence of the dielectric susceptibility under various electric fields for $x=0.005$.

about 13 K for $x=1.0$, in good agreement with the experimental value.¹²

Figure 2(a) lists the experimental T_C within the whole concentration of $0 \leq x \leq 1$,⁹⁻¹¹ where our theoretical concentration dependence of T_C can well reproduce the experimental data with the remaining discrepancy due to the grain size effect in the real material system. We note that T_C varies linearly with x for high concentrations, and deviates gradually from the linear behavior at low concentrations, which, in our view, can be attributed to the quantum effect on the ferroelectricity of BST (this will be discussed in detail below). With the further decrease in the impurity concentration, as Fig. 2(b) shows, the concentration dependence of T_C will exhibit special behavior induced by the quantum effect in the concentration range slightly higher than x_C : $T_C=C(x-x_C)^{1/2}$ (Refs. 12–14) with C a constant.

It should be noted that x_C was reported to be around 0.035,¹² 0.01,¹³ 0.0002,¹⁴ 0.005,³² and 0.09.³³ This extremely high scatter of the data shows that impurity-induced ferroelectric phase transition strongly depends on the details of growth technology and on the purity of starting chemical materials. Our theoretical calculation gives x_C to be 0.0096, in good agreement with the experimental result of 0.01 reported in Ref. 13. Furthermore, it is clear that our theoretical concentration dependence of T_C [the solid curve in Fig. 2(b)] also demonstrates well the predicted empirical relation of $T_C=C(x-x_C)^{1/2}$ with $C=270$. Below we will further show that for impurity concentration close to x_C , BST changes from a quantum paraelectric ($0 \leq x \leq x_C$) to a quantum ferroelectric ($x_C < x < 0.1$), where BST exhibits the feature of normal ferroelectrics (i.e., there is a dielectric peak at T_C in the temperature dependence of the dielectric susceptibility) with quantum effect.

It is well known that with the increase of the electric field the dielectric maximum temperature $T_m(E)$ of ferroelectric materials will shift to high temperatures due to the electric-field-induced polarization. But detailed explanation on the electric field dependence of $T_m(E)$ is not available so far for

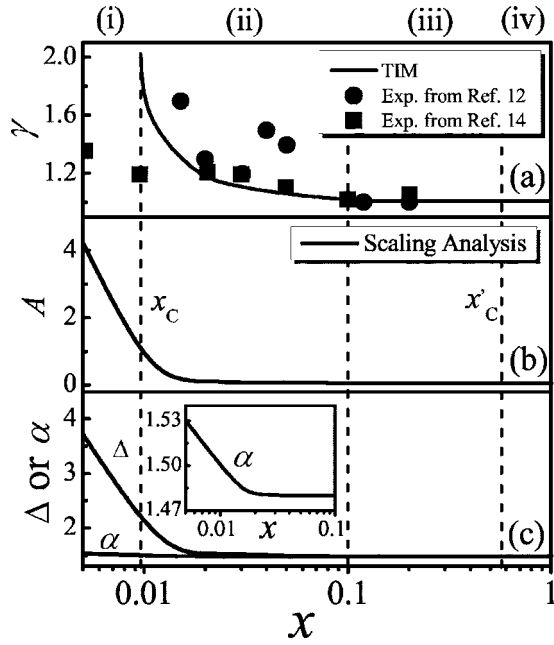


FIG. 4. Concentration dependence of the (a) exponent γ , (b) coefficient A , and (c) exponents Δ and α . Sections (i–iv) correspond to regimes of the quantum paraelectric ($0 \leq x \leq x_c = 0.0096$), quantum ferroelectric ($x_c < x < 0.1$), classic ferroelectric with second-order phase transition ($0.10 \leq x < x'_c = 0.57$), and classic ferroelectric with first-order phase transition ($0.57 \leq x \leq 1.0$), respectively. The inset of (c) is the enlarged concentration dependence of α below $x = 0.1$.

BST system with various impurity concentrations. Here we define $\Delta T_m(E)$ the difference between the nonzero-field dielectric maximum temperature $T_m(E)$ and zero-field dielectric maximum temperature T_C . Figure 3(a) shows the electric field dependence of $\Delta T_m(E)$ for x slightly higher than x_c ($0.01 \leq x < 0.1$), where the BST system exhibits the feature of quantum ferroelectrics. It is clear that with the increase of the impurity concentration the effect of the electric field on $\Delta T_m(E)$ is reduced. The increased dipole moment interaction and reduced quantum effect result in the increase of the electric polarization, and consequently the effect of the electric field on the polarization is reduced. We therefore expect the decrease of the electric-field-induced polarization, which requires small temperature variation to conquer the ferroelectric ordering induced by the electric field. Another remarkable feature in Fig. 3(a) is that $\Delta T_m(E)$ increases with the electric field much more rapidly at lower impurity concentration (near x_c) than that at higher ones. This is reasonable, since the quantum suppression over polarization (and therefore the effect of electric field on polarization) decreases rapidly with the increase of impurity concentrations.

For the BST with impurity concentration smaller than x_c , the dielectric behavior exhibits the feature of the quantum paraelectrics under zero electric field, i.e., without showing a dielectric maximum, as shown in Fig. 1. Under an electric field, however, a round dielectric peak can be observed near a threshold electric field E_C [~ 223 KV/m for $x = 0.005$, see the inset of Fig. 3(b)], indicating the onset of the induced ferroelectric order, and the peak is found to shift to high

temperature with the increase of the electric field, as shown in the phase diagram of Fig. 3(b). The peak maxima separate the paraelectric regime (low-polarization state) at high temperatures and low fields from the induced ferroelectric regime (high-polarization state) at low temperatures and high electric fields. The inset of Fig. 3(b) also reveals that due to the large quantum fluctuations, the high polarization state is still characterized by a large amount of disorder and consequently yields high dielectric response in the ferroelectric regime.

With the consideration of the quantum effect, dielectric susceptibility of BST in the paraelectric phase can be expressed as: $1/\chi_0(T) \propto (T - T_C)^\gamma$,¹⁴ where the critical exponent γ is important for scaling the quantum effect and $\gamma = 1$ corresponds to the classical case. We have displayed in Fig. 4(a) the critical exponent γ as a function of impurity concentration x . It is found that, with the decrease of the impurity concentration, γ gradually deviates from the classical value of 1 at the impurity concentration $x = 0.10$ and increases rapidly near the critical concentration $x_c = 0.0096$ (corresponding to the rapid increase of the quantum suppression over polarization), in agreement with the experimental results reported in Refs. 12 and 14. The fact that γ reaches 2 at x_c indicates a dramatic increase of the quantum effect on dielectric susceptibility, although BST begins to show the behavior of normal ferroelectrics as displayed in Fig. 1 at this concentration. As a result, we can define two quantum regimes within $0 \leq x < 0.10$ in BST, with quantum paraelectric region of $0 \leq x \leq x_c = 0.0096$ [Sec. (i) in Fig. 4, where the system exhibits the behavior of normal quantum paraelectrics] and quantum ferroelectric one of $x_c < x < 0.1$ [Sec. (ii) in Fig. 4, where the BST shows the behavior of normal ferroelectrics under the domination of quantum mechanical effect]. In the quantum region, T_C varies with x via $T_C = 270(x - x_c)^{1/2}$ above x_c , rather than the linear relation in the classical region of $0.10 \leq x \leq 1.0$ [Secs. (iii) and (iv) in Fig. 4].

The above dielectric behavior originates from the competition between the dipole moment interaction and quantum mechanical tunneling, and can be explained in a certain microscopic mechanism with the quantity $J/2\Omega$ to scale the quantum effect. The critical concentration x_c corresponds to the case of $J/2\Omega = 1$. With the increase of impurity concentration, the nearest-neighbor pseudospin interaction gradually dominates over the quantum fluctuation, leading to the transition from a paraelectric at $J/2\Omega < 1$ to a ferroelectric at $J/2\Omega > 1$. Moreover, the increase of $J/2\Omega$ will cause the reduction of the quantum effect on the dielectric behavior, until the disappearance of the quantum effect at $J/2\Omega = 1.8$ in BST with $x = 0.10$.

We can qualitatively describe the quantum effect in BST by employing the static nonzero-external-field scaling analysis^{22,23} to fit the electric field dependence $\Delta T_m(E)$ in Fig. 3. Due to the existence of threshold electric field E_C and $T_C = 0$ K, we have modified the scaling theory formula Eq. (7) as $T_m(E) = A(E - E_C)^{1/\Delta}$ for $x < x_c$. It is clear that our theoretical results within the framework of the TIM can fit well with the scaling theory formula. Figures 4(b) and 4(c) list the yielded coefficients A and gap exponents Δ throughout the impurity concentrations, which also demonstrate the role of quantum effect in BST, i.e., at low concentrations they rap-

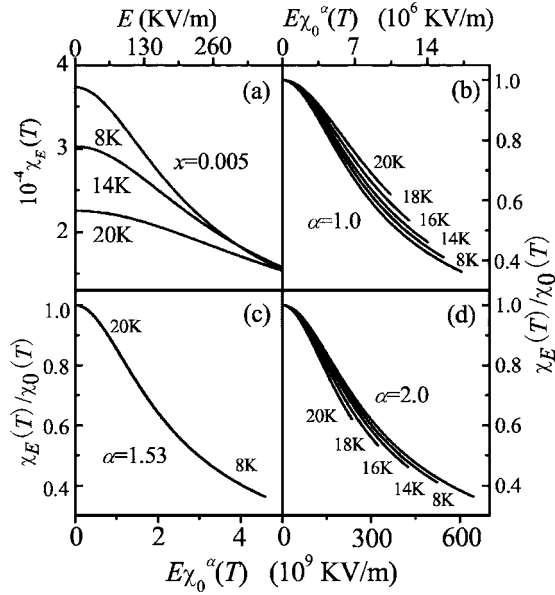


FIG. 5. (a) Electric field dependence of $\chi_E(T)$ at various temperatures for $x=0.005$, and dependence of $\chi_E(T)/\chi_0(T)$ on $E\chi_0^\alpha(T)$ for $x=0.005$ with (b) $\alpha=1.0$, (c) $\alpha=1.53$, and (d) $\alpha=2.0$, revealing the best collapsing data under $\alpha=1.53$.

idly deviate from the classical results, similar to the concentration dependence of γ . Furthermore, in addition to the reflection of the quantum effect, the magnitude of the coefficient A is also directly associated with the role of electric field on $T_m(E)$. Since impurity doped ferroelectric systems usually can be well described by scaling analysis, our present method allows us to obtain a more comprehensive understanding of these systems.

The scaling relation of Eq. (6) was originally derived for ferroelectric systems in the vicinity of their critical points.²³ By examining the effect of electric field on dielectric susceptibility in the paraelectric system with large quantum fluctuation, we can also manifest the quantum effect in BST through applying the scaling relation of Eq. (6) to the dielectric ratio $\chi_E(T)/\chi_0(T)$. Figure 5(a) displays the isotherms $\chi_E(T=const)$ of BST with very low concentration of $x=0.005$ at low temperatures. A monotonic decay of dielectric susceptibility is observed with the increase of the electric field, which is related to the considerable nonlinearity caused by the dipole moment interaction. With the increase of temperature, the electric field has a decreasing effect on the dielectric susceptibility due to the increasing disorder.

To check the scaling behavior of the TIM deduced data, we show in Figs. 5(b)–5(d) the ratio $\chi_E(T)/\chi_0(T)$ versus $E\chi_0^\alpha(T)$ at $8 \leq T \leq 20$ K and $0 \leq E \leq 460$ KV/m under different values of α . It is clear that the best data collapsing onto one uniform function occurs in the case of $\alpha=1.53$, where the effect of electric field on the dielectric susceptibility can be simply obtained only with *a priori* knowledge of $\chi_0(T)$. We have further displayed in Fig. 4(c) the yielded α in BST within the whole concentration range. It is noted that a classical exponent α of 1.48 has been observed in the classical ferroelectric regime of $0.10 \leq x \leq 1.0$. The inset of Fig. 4(c) shows the enlarged variation of α with x , indicating the rapid

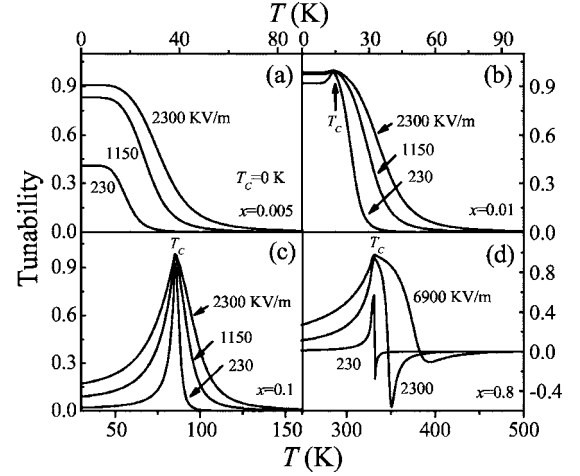


FIG. 6. Temperature dependence of the tunability in BST with (a) $x=0.005$, (b) $x=0.01$, (c) $x=0.1$, and (d) $x=0.8$ under various electric fields.

decrease of the quantum fluctuation for BST from a quantum paraelectric to a quantum ferroelectric. In addition, according to the scaling theory, the ratio of Δ to α is related to the exponent γ . The rapid decrease of the ratio (Δ/α) in Fig. 4(c) with the increase of impurity concentration also demonstrates the variation of quantum effect within the BST system.

It is well known that the tunability in ferroelectric materials is an important physical quantity to scale the effect of the electric field on the dielectric constant, and can be expressed as: $\frac{\chi_0(T) - \chi_E(T)}{\chi_0(T)}$.³⁴ We show in Fig. 6 that the tunability in BST displays quite different features with different impurity concentrations as a result of the phase transition and quantum effect. Figure 6(a) presents the temperature dependence of the tunability under various electric fields in the quantum paraelectric regime ($x=0.005$). With the increase of temperature, the large quantum suppression decreases, resulting in the gradual deviation of the tunability from saturation at very low temperatures. The increase of the electric field will greatly enhance the tunability due to the increased reduction of the dielectric susceptibility. It should be noted that, although there exists a round peak under an electric field higher than E_C in the temperature dependence of the dielectric property (the inset of Fig. 3), we cannot observe the peak caused by the electric-field-induced ordering state in the tunability characteristics, further indicating that the appearance of the round peak does not correspond to the phase transition.

For impurity concentration in the quantum ferroelectric regime, the feature of the tunability [Fig. 6(b)] is quite different from that in the quantum paraelectric regime. It is shown that there is an evident peak in the temperature dependence of the tunability, and the peak broadens with the increase of the electric field, indicating the ferroelectric phase transition in the system. In the very low temperature range of $T < T_C$, the tunability keeps a high value and is approximately temperature independent, similar to the quantum paraelectric case [Fig. 6(a)]. It is the remaining quantum suppression over the spontaneous polarization that makes the

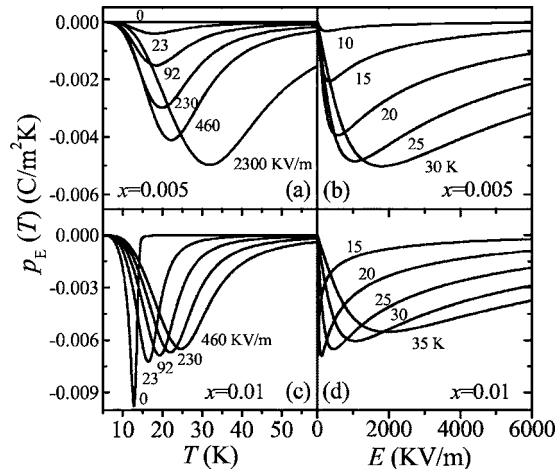


FIG. 7. (a) Temperature and (b) electric field dependence of the pyroelectric coefficient in the quantum paraelectric regime of $x=0.005$; (c) Temperature and (d) electric field dependence of the pyroelectric coefficient in the quantum ferroelectric regime of $x=0.01$.

zero-field dielectric constant greatly enhanced. Nevertheless, in the case of the classical regime [Fig. 6(c), Sec. (iii) in Fig. 4], since the quantum effect is greatly reduced, the very small low- T tunability has an evident increase with the temperature, and reaches ~ 1 (saturation tunability) at T_C . Consequently, a very sharp peak at T_C can be observed in the tunability characteristics due to the ferroelectric phase transition,³⁴ and the peak broadens with the increase of the electric field. The fact that the dielectric susceptibility decreases with the increase of electric fields in the whole examined temperature range further indicates that the phase transition is of second order. Furthermore, we note that our tunability results of Fig. 6(c) qualitatively agree with experiments for a concentration of $x=0.8$ in Ref. 34. This is due to the fact that the experimental data in Ref. 34 are from BST ceramics (ferroelectric polycrystalline). The average effect of the phase transition in BST polycrystalline can only display the continuous second-order phase transition, rather than the discontinuous first-order transition. Therefore, the observed experimental tunability in Ref. 34 exhibits the second-order phase transition behavior, though the concentration of $x=0.8$ is within our predicted first-order phase transition region in ideal single crystalline BST system.

With the further increase of the impurity concentration [higher than $x'_C=0.57$, Sec. (iv) in Fig. 4], as Fig. 6(d) shows, in addition to the sharp peak at T_C [similar to that of Fig. 6(c)] due to the phase transition, we can observe a tunability minimum with negative values at the temperature slightly higher than T_C . The increase of the dielectric susceptibility under electric fields in the paraelectric state indicates that there is an electric-field-induced phase transition at this concentration, i.e., the phase transition in BST with $x \geq 0.57$ is of first order. This conclusion is in good agreement with the evident reduction of the zero-field dielectric maximum from $x=0.6$ to 1.0 in Fig. 1. With the increase of the electric field, though both the tunability peak and minimum broaden, the tunability peak does not change with the electric field, while the tunability minimum is found to shift to high tempera-

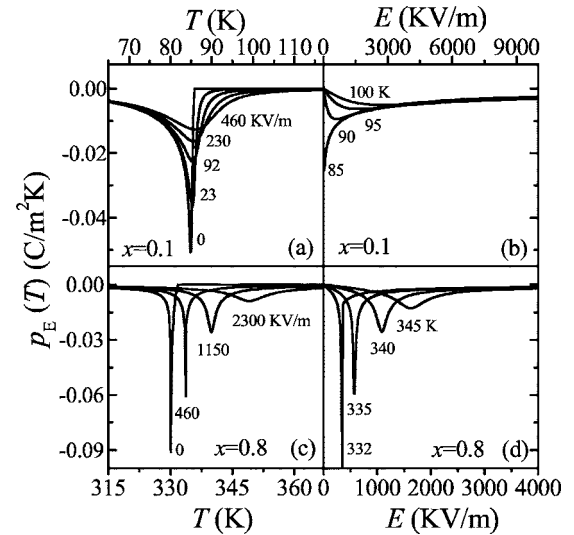


FIG. 8. (a) Temperature and (b) electric field dependence of the pyroelectric coefficient in the classic ferroelectric regime ($x=0.1$, with the second-order phase transition); (c) Temperature and (d) electric field dependence of the pyroelectric coefficient in the classic ferroelectric regime ($x=0.8$, with the first-order phase transition).

tures. This is due to the competition between the thermo-perturbation and electric field, which also results in the observed nonmonotonic behavior of the tunability minimum.

Now, we move our attention to the pyroelectric properties in the BST system. As we know the pyroelectric behavior scales the response of the electrical polarization to the temperature and therefore, is also associated with the phase transition and quantum effect. We present in Figs. 7 and 8 the pyroelectric characteristics in BST with different impurity concentrations under various electric fields and temperatures. Because of the large quantum fluctuation in the quantum paraelectric regime ($0 \leq x \leq x_C$), Fig. 7(a) shows that the thermo-perturbation has little effect on the polarization under zero electric field. Application of an electric field will induce the competition between the thermo-perturbation and polarization. Therefore, with the increase of the temperature, a maximum pyroelectric effect (pyroelectric minimum) on the polarization will be observed at a certain temperature. With the increase of the electric field, the pyroelectric effect will be enhanced at low electric field due to the increased polarization. Further increase of the electric field, however, will weaken the pyroelectric effect due to the saturation of the electric-field-induced polarization under a certain high field [Fig. 7(b)].

It is clear that the temperature and electric field dependences of the pyroelectric characteristics in the quantum ferroelectric regime [Figs. 7(c) and 7(d)] are quite different from those in Figs. 7(a) and 7(b). On one hand, under zero electric field, a rapid variation of the pyroelectric effect occurs at T_C , corresponding to the phase transition in the system. On the other hand, due to the existence of the spontaneous polarization, the effect of the electric field dominates over the thermo-perturbation at low temperatures, resulting in the saturation of polarization. As a result, the pyroelectric

effect will decrease with the increase of electric field below T_C . Nevertheless, at high temperatures, the pyroelectric effect increases with the electric field at both these two quantum regimes as a result of the increased polarization.

Figure 8 displays the pyroelectric characteristics of BST in the classical ferroelectric regime, i.e., without quantum effect there. At concentrations below $x'_C=0.57$ [Figs. 8(a) and 8(b)], the temperature of the pyroelectric minimum remains almost unchanged and broadens in shape with the increase of the electric field, further indicating that the phase transition at this concentration is of second order³⁵ [consistent with the tunability behavior in Fig. 6(c)]. In comparison with the temperature dependence of the pyroelectric behavior at low concentrations, the pyroelectric effect in BST with concentration above $x'_C=0.57$ [Figs. 8(c) and 8(d)] shows a more rapid increase with the temperature below T_C under zero electric field. This indicates that there is a sudden decrease of the polarization near T_C , and even at the temperature slightly higher than T_C , the sharp pyroelectric minimum can still be observed under an electric field. This kind of field-induced phase transition will disappear with the further increase of the electric field, where the pyroelectric minimum is found to shift to high temperatures, broaden in shape and become weak, as a result of high thermo-perturbation. The above arguments demonstrate again the first-order phase transition nature³⁶ of BST at this concentration.

Finally, we discuss the role of the quantum effect on the electric field dependence of the pyroelectric coefficient. In the paraelectric regime with strong quantum effect [Figs. 7(a) and 7(b)], the absolute value of the pyroelectric minimum increases with the electric field. With the decrease of the quantum effect, the pyroelectric minimum changes little with the electric field in the quantum ferroelectric regime [Figs. 7(c) and 7(d)]. In contrast, in the classic ferroelectric regime (Fig. 8), the lack of quantum effect will result in the decrease of the absolute value of the pyroelectric minimum with the increase of the electric field. This can be simply understood by the fact that the quantum suppression over the electric-field-induced polarization decreases rapidly with the increase of the concentration in BST system. The easy saturation of the polarization in BST system will lead to the decreasing dependence of the thermo-perturbation with the increase of electric fields.

As for the comparison with the experiments, most of the experimental pyroelectric properties reported in the literature concern the BST thin films and graded materials, it is difficult to have a direct comparison with our present theoretical

results in ideal BST bulk system. In fact, a complete physical picture of doping concentration and electric field dependence of the pyroelectric properties in BST is still unavailable experimentally. There is also no experimental report on the relation of the electric field dependent pyroelectric properties with the quantum effect and phase transition. We hope that our present detailed theoretical work can stimulate the related experimental research in BST.

IV. CONCLUSIONS

We have shed light on the dielectric and pyroelectric properties in BST system within the whole concentration range through the application of the TIM, with the consideration of the cell volume effect and ferroelectric distortion. By investigating in detail the electric field dependence of the dielectric and pyroelectric characteristics, we have clearly demonstrated the quantum effect and phase transition in BST with various impurity concentrations. It is found that the results within the framework of the TIM can well fit with the scaling theory, which usually can be used to analyze the dielectric properties in ferroelectric systems, giving an applicable way to have further understanding on the nature of the quantum effect and phase transition. We have classified four regimes in BST within the whole concentration range: (i) The quantum paraelectric regime for $0 \leq x \leq x_C=0.0096$, where the dielectric and pyroelectric behavior are dominated by the dramatic quantum effect that keeps the system a paraelectric even at very low temperatures; (ii) the quantum ferroelectric one for $x_C < x < 0.1$, where ferroelectric phase transition occurs in BST under a remaining quantum effect; (iii) $0.1 \leq x < 0.57$ for the classical ferroelectric region, where the quantum effect disappears and phase transition is of second order; and (iv) $0.57 \leq x \leq 1.0$ for another classical ferroelectric one with the phase transition of first order. The revealed interesting concentration-dependent dielectric and pyroelectric phenomena provide a theoretical basis for further experimental exploration and device design of BST system.

ACKNOWLEDGMENT

This work was supported by the Natural Science Foundation of China under Contract Nos. 10125416 and 60576067 and the National Minister of Education Program for Changjiang Scholars and Innovative Research Team in University (PCSIRT).

*Corresponding author. Email address: wzshen@sjtu.edu.cn

¹F. Jona and G. Shirane, *Ferroelectric Crystals* (Dover, New York, 1993).

²M. E. Lines and A. M. Glass, *Principles and Applications of Ferroelectrics and Related Materials* (Oxford University Press, New York, 1977).

³B. Jaffe, W. R. Cook, and H. Jaffe, *Piezoelectric Ceramics* (Academic, New York, 1971).

⁴G. A. Smolensky, V. A. Bokov, V. A. Isupov, N. N. Kranik, R. E. Pasynkov, A. I. Sokolov, and N. K. Yushin, *Ferroelectrics and Related Materials* (Gordon and Breach, New York, 1984).

⁵S. Ezhilvalavan and T. Y. Tseng, *Mater. Chem. Phys.* **65**, 227 (2000).

⁶C. M. Carlson, T. V. Rivkin, P. A. Parilla, J. D. Perkins, D. S. Ginley, A. B. Kozyrev, V. N. Oshadchy, and A. S. Pavlov, *Appl. Phys. Lett.* **76**, 1920 (2000); P. C. Joshi and M. W. Cole, *ibid.*

- 77, 289 (2000).
- ⁷K. A. Müller and H. Burkard, *Phys. Rev. B* **19**, 3593 (1979).
- ⁸J. G. Bednorz and K. A. Müller, *Phys. Rev. Lett.* **52**, 2289 (1984).
- ⁹D. A. Tenne, A. Soukiassian, X. X. Xi, H. Choosuwan, R. Guo, and A. S. Bhalla, *Phys. Rev. B* **70**, 174302 (2004), and references therein.
- ¹⁰R. Naik, J. J. Nazarko, C. S. Flattery, U. D. Venkateswaran, V. M. Naik, M. S. Mohammed, G. W. Auner, J. V. Mantese, N. W. Schubring, A. L. Micheli, and A. B. Catalan, *Phys. Rev. B* **61**, 11367 (2000).
- ¹¹L. Q. Zhou, P. M. Vilarinho, and J. L. Baptista, *J. Eur. Ceram. Soc.* **19**, 2015 (1999).
- ¹²V. V. Lemanov, E. P. Smirnova, P. P. Syrnikov, and E. A. Tarakanov, *Phys. Rev. B* **54**, 3151 (1996).
- ¹³V. V. Lemanov, *Ferroelectrics* **302**, 169 (2004).
- ¹⁴R. Wang, Y. Inaguma, and M. Itoh, *Mater. Res. Bull.* **36**, 1693 (2001).
- ¹⁵K. C. McCarthy, F. S. McCarthy, G. Teowee, T. J. Bukowski, T. P. Alexander, and D. R. Uhlmann, *Integr. Ferroelectr.* **17**, 377 (1997).
- ¹⁶C. Hanson and H. Beratan, *Proc. 9th International Symposium on Applied Ferroelectrics* (IEEE, New York, 1994), p. 657.
- ¹⁷J. Hemberger, M. Nicklas, R. Viana, P. Lunkengeimer, A. Liodl, and R. Böhmer, *J. Phys.: Condens. Matter* **8**, 4673 (1996).
- ¹⁸H. Wu, Q. Jiang, and W. Z. Shen, *Phys. Rev. B* **69**, 014104 (2004).
- ¹⁹J. Barret, *Phys. Rev.* **86**, 118 (1952).
- ²⁰B. Zalar, A. Lebar, J. Seliger, R. Blinc, V. V. Laguta, and M. Itoh, *Phys. Rev. B* **71**, 064107 (2005).
- ²¹H. Wu and W. Z. Shen, *Appl. Phys. Lett.* **87**, 252906 (2005).
- ²²B. Westwanski, B. Fugiel, A. Ogaza, and M. Pawlik, *Phys. Rev. B* **50**, 13118 (1994).
- ²³B. Westwanski and B. Fugiel, *Phys. Rev. B* **43**, 3637 (1991).
- ²⁴L. Zhang, W. Zhong, Y. G. Wang, and P. L. Zhang, *Solid State Commun.* **104**, 263 (1997).
- ²⁵L. Zhang, W. Kleemann, and W. Zhong, *Phys. Rev. B* **66**, 104105 (2002).
- ²⁶W. R. Buessem, L. E. Cross, and A. K. Goswami, *J. Am. Chem. Soc.* **49**, 33 (1966).
- ²⁷S. Minomura, M. Tanaka, B. Okai, and H. J. Nagasaki, *J. Phys. Soc. Jpn.* **28s**, 404 (1970).
- ²⁸D. Berlincourt and H. Jaffe, *Phys. Rev.* **111**, 143 (1958).
- ²⁹L. Zhang, W. Zhong, and W. Kleemann, *Phys. Lett. A* **276**, 162 (2000).
- ³⁰V. V. Lemanov, A. V. Sotnikov, E. P. Smirnova, M. Weihnacht, and R. Kunze, *Solid State Commun.* **110**, 611 (1999).
- ³¹O. E. Kvyatkovskii, *Phys. Solid State* **43**, 1401 (2001).
- ³²J. G. Bednorz, Ph.D. Thesis, Swiss Federal Institute of Technology, Zürich (1982).
- ³³C. Ménoret, J. M. Kiat, B. Dkhil, M. Dunlop, H. Dammak, and O. Hernandez, *Phys. Rev. B* **65**, 224104 (2002).
- ³⁴X. Y. Wei and X. Yao, *Mater. Sci. Eng., B* **99**, 74 (2003).
- ³⁵A. F. Devonshire, *Adv. Phys.* **3**, 85 (1954).
- ³⁶R. Poprawski, *Ferroelectrics* **33**, 23 (1981).